

Chronos^{*}

A NIR Spectroscopic Galaxy Survey: From the formation of galaxies to the peak of activity

IGNACIO FERRERAS^{1†}, RAY SHARPLES²

Science Core Team

JAMES S. DUNLOP³, ANNA PASQUALI⁴, FRANCESCO LA BARBERA⁵, ALEXANDER VAZDEKIS⁶,
SADEGH KHOCHFAR³, MARK CROPPER¹, ANDREA CIMATTI⁷, MICHELE CIRASUOLO^{3,8},

RICHARD BOWER², JARLE BRINCHMANN⁹, BEN BURNINGHAM¹⁰, MICHELE CAPPELLARI¹¹,
STÉPHANE CHARLOT¹², CHRISTOPHER J. CONSELICE¹³, EMANUELE DADDI¹⁴, EVA K. GREBEL⁴,
ROB IVisON^{3,8}, MATT J. JARVIS¹¹, DAISUKE KAWATA¹, ROBERT C. KENNICUTT¹⁵,
TOM KITCHING¹, OFER LAHAV¹⁶, ROBERTO MAIOLINO¹⁵, MATHEW J. PAGE¹,
REYNIER F. PELETIER¹⁷, ANDREW PONTZEN¹⁶, JOSEPH SILK¹², VOLKER SPRINGEL^{4,18},
MARK SULLIVAN¹¹, IGNACIO TRUJILLO⁶, GILLIAN WRIGHT⁸

Submitted to ESA, May 24th, 2013
<http://www.chronos-mission.eu>



¹ Mullard Space Science Laboratory, University College London, UK; ² University of Durham, UK; ³ Royal Observatory, University of Edinburgh, UK; ⁴ ARI/ZAH, University of Heidelberg, Germany; ⁵ INAF/OAC, Naples, Italy; ⁶ Instituto de Astrofísica de Canarias, Spain; ⁷ Università di Bologna, Italy; ⁸ UK ATC, Edinburgh, UK; ⁹ Leiden University, the Netherlands; ¹⁰ University of Hertfordshire, UK; ¹¹ Oxford University, UK; ¹² Institut d'Astrophysique de Paris, France; ¹³ Nottingham University, UK; ¹⁴ CEA/Saclay, France; ¹⁵ Institute of Astronomy, University of Cambridge, UK; ¹⁶ Physics & Astronomy Department, University College London, UK; ¹⁷ Kapteyn Institute, University of Groningen, the Netherlands; ¹⁸ Heidelberg Institute for Theoretical Studies, Germany.

^{*}Chronos, the Greek god personifying time is the name we have given to this survey, as it is designed to understand the formation and evolution of galaxies across cosmic time

[†]i.ferreras@ucl.ac.uk

Executive Summary

In a decade or two from now, we will have made significant strides in our understanding of the early formation history of the Universe, through missions such as *Planck* and *Euclid*, and in its recent state, through *Gaia* and ground-based surveys such as SDSS and their more substantial successors. What will still be problematic is how we arrived here given the initial conditions. This is the realm of “baryon physics”, the nature of the formation and evolution of the galaxies. Understanding this is a colossal task, currently occupying a large fraction of the international astronomical community. It involves complex astrophysics at redshifts 1–6. To make the critical and substantial advances in our understanding of the essential nature of this process requires spectroscopy (for the astrophysics) in the infrared (because of the redshift) of a large volume of the Universe (to examine the critical effects of environment). This is what the concept presented here sets out to achieve.

We propose *Chronos*, an L-class mission to understand the formation and evolution of galaxies, by collecting the deepest NIR spectroscopic data, from the formation of the first galaxies at $z \sim 10$ to the peak of formation activity at $z \sim 1-3$. The strong emission from the atmospheric background makes this type of survey impossible from a ground-based observatory. The spectra of galaxies represent the equivalent of a *DNA fingerprint*, containing information about the past history of star formation and chemical enrichment. The proposed survey will allow us to dissect the formation process of galaxies including the timescales of quenching triggered by star formation or AGN activity, the effect of environment, the role of infall/outflow processes, or the connection between the galaxies and their underlying dark matter haloes. To provide these data, the mission requires a 2.5m space telescope optimised for a campaign of very deep NIR spectroscopy. A combination of a high multiplex and very long integration times will result in the deepest, largest, high-quality spectroscopic dataset of galaxies from $z=1$ to 12, spanning the history of the Universe, from 400 million to 6 billion years after the big bang, i.e. covering the most active half of cosmic history.

The highly demanding requirements results in a mission that is the spectroscopic equivalent of a *Hubble Space Telescope* obtaining one Ultra Deep Field (the deepest exposure of distant galaxies ever attained) every fortnight for five years. A two-tiered survey will provide a high quality stellar mass limited dataset of about 2 million spectra from galaxies covering the most important epochs of structure formation, back to the early phases soon after recombination. Although missions such as *Euclid* or *WFIRST* will provide low-resolution spectra in the NIR, the requirements of resolution and SNR in the continuum for the analysis of the properties of the underlying stellar populations at $z \lesssim 3$ are too demanding for them. Therefore, *Chronos* is the link between cosmology-orientated missions, such as *Planck* or *Euclid* and *Gaia*'s targeted exploration of our own galaxy. Our mission will gather key spectroscopic indicators of the properties of the underlying stellar populations in galaxies. This will be complemented by *Herschel*'s view of the “dusty” side of the Universe.

The survey will allow us to understand the most fundamental open questions in galaxy formation today: the connection between the star formation and the mass assembly history of galaxies; the interplay of star formation and activity from a central supermassive black hole in shaping the properties of galaxies; the connection between chemical composition and the formation histories of galaxies (“extragalactic archaeology”); and the contribution of the environment and the pervading dark matter halos to the formation of galaxies.

The main science questions that the mission will answer are:

- The connection between the star formation history and the mass assembly history.
- The role of AGN and supernova feedback in shaping the formation histories of galaxies, with a quantitative estimate of quenching timescales.
- The formation of the first galaxies.
- The source of reionization.
- Evolution of the metallicity-mass relation, including $[\alpha/\text{Fe}]$ and individual abundances.
- Initial Mass Function as a tracer of star formation modes.

I. A NATURAL CHOICE FOR THE NEXT L-CLASS MISSION

Even though astronomy as a human activity goes back to the origins of civilization, and the understanding of celestial bodies has been responsible for the scientific method that led to our technology-based society, some of the most fundamental aspects of this scientific discipline remain largely unsolved. It was less than a century ago that we began to understand the true meaning of galaxies as “Universe islands”, and even more recently that we could put them in context with the underlying dark matter backbone and the evolution of the Universe as a whole. The luminous component of galaxies is dominated by stars, gas and dust. This L-class mission is designed to address one of the major questions in ESA’s “COSMIC VISION 2015-2025” BR-247 document, namely question 4: **How did the Universe originate and what is it made of?**, and especially topic 4.2: **The Universe taking shape.**

Two of ESA’s recent cornerstone missions concentrate on very specific – and essential – aspects of this problem, namely the evolution of the dust in star forming galaxies (*Herschel*) and the history of our own Milky Way galaxy (*Gaia*). The global structure and evolution of the Universe is the main target of ESA’s *Planck* and *Euclid* missions. Now, the next Large mission should tackle the much wider problem of understanding the “baryon physics” of galaxy formation, namely the highly complex set of physical mechanisms responsible for the transformation of the primordial hydrogen and helium gas mixture into the galaxies we see today. At a more fundamental level, it is possible to understand the nature of dark matter only if we have a comprehensive understanding of galaxy formation. Such an endeavour requires the highest quality spectroscopic dataset over a large survey, probing two major cosmic epochs: a) the epoch at the peak of galaxy formation activity, namely between redshifts $z \sim 3$ and 1 (i.e. 2 and 6 billion years after the Big Bang), and b) the formation of the first galaxies, at redshifts between $z=12$ and 6 (between 400 and

900 million years after the Big Bang). The spectroscopic analysis of galaxies constitutes the equivalent of DNA fingerprinting, allowing us to determine the composition of the galaxy and its past formation history.

Even though ongoing and future surveys, such as *Euclid*, *WFIRST*, *LSST* or *SKA*¹ will give insightful clues about the origins of galaxies, high quality spectroscopic data at moderately high resolution ($R \equiv \lambda/\Delta\lambda \approx 1,000 - 2000$) is the *only* way that this problem can be solved. While ground-based NIR spectroscopy will undoubtedly make important strides in the coming decades, OH and other backgrounds inherent to ground based NIR spectroscopy will ensure that the spectroscopic performance of *Chronos* – at the faintness levels and spectral coverage required for this science – will remain unchallenged. The behemoths of astronomical science in the coming decades (*JWST* from space or the *E-ELT* from the ground) will, in all likelihood, target in detail specific issues of this project, but their very limited field of view makes them incapable of gathering anywhere near the scale of dataset required to make the extensive advances *Chronos* will deliver in the area of galaxy formation and evolution. Rather than a competitor, ultra-large observing facilities will be a complement to *Chronos*.

Chronos in a nutshell

Chronos is a dedicated 2.5m space telescope optimized for ultra-deep NIR spectroscopy at moderate resolution ($R=1500$) in the 0.9-1.8 μm range. The 5-year long, two-tiered survey will reach $H_{\text{AB}}=26$ over a 100 deg², and $H_{\text{AB}}=27.2$ over 10 deg² at a 5σ level in the continuum. The two main science drivers are the formation of galaxies at the peak of activity ($1 < z < 3$) and the first galaxies and the source of reionization ($z > 6$).

II. THE EVOLUTION OF GALAXIES AT THE PEAK OF ACTIVITY

II.1 Introduction

Over the past two decades, advances in detector technology have allowed us to probe the evolution of star formation with cosmic time (Fig. 1, left panel). Between the formation

of the first galaxies and the present time, there was an epoch when the global star formation history was at its peak, in the redshift interval between $z \sim 3$ and 1. During this epoch, the majority of the stars in the present Universe were formed and assembled into galaxies, making it

¹Although *SKA* will deliver an unprecedented map of the first stages of structure formation, its design will only target the gas component through observations of the HI 21 cm line.

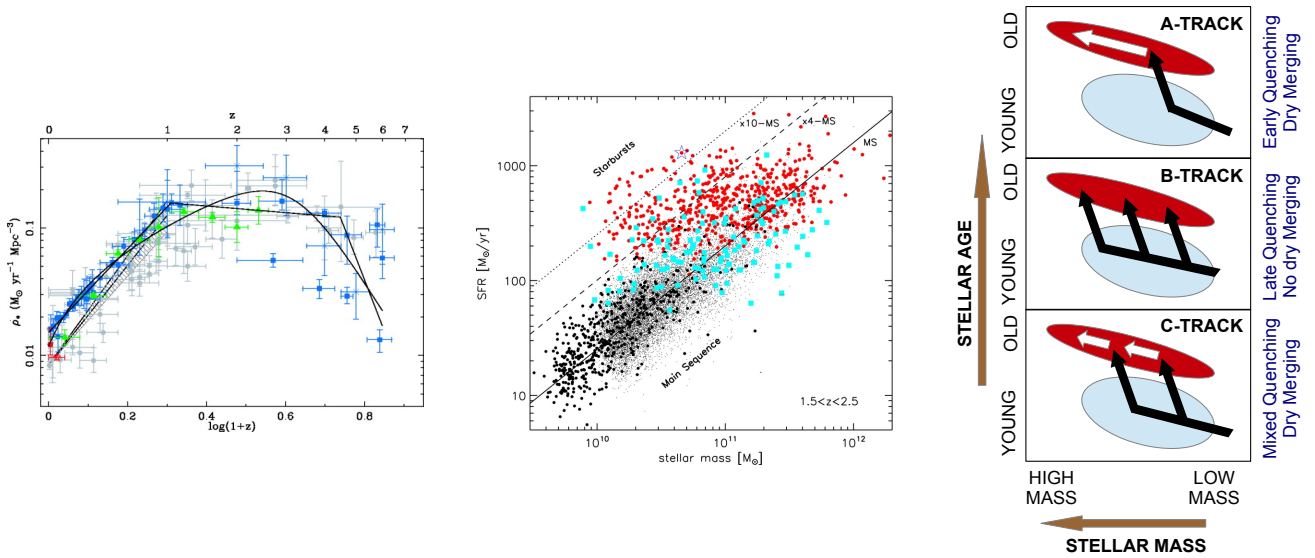


Figure 1: **Left:** Cosmic star formation history (from Hopkins & Beacom, 2006). **Middle:** Different modes of star formation (from Rodighiero *et al.*, 2011)). **Right:** Schematics of galaxy evolution from the blue cloud to the red sequence (adapted from Faber *et al.*, 2007).

– along with the very first epoch of galaxy formation (see Sec. III) – the most important interval of cosmic history. In the “local” Universe (i.e. $z \lesssim 0.1$), large spectroscopic surveys, most notably the Sloan Digital Sky Survey (hereafter SDSS, York *et al.*, 2000) provided enough data to trigger a quantum leap in our understanding of galaxy formation. In the post-SDSS era it is possible to dissect datasets according to various properties such as stellar mass, velocity dispersion, morphology, environment, enabling us to “ask the right questions”. SDSS has shown that gathering a *complete* database comprising up to a million spectra is necessary to constrain in detail the many aspects that contribute to the process of galaxy formation. The spectroscopic analysis of the stellar populations in the SDSS Universe confirmed in exquisite detail the strong bimodality between passive, and predominantly massive galaxies (the so-called *red sequence*) and a *blue cloud* of star forming systems (Baldry *et al.*, 2004). Furthermore, SDSS also revealed the presence of a characteristic mass scale in the local Universe, around 3×10^{10} solar masses in stars (Kauffmann *et al.*, 2003), which marks a clear transition in the baryon content of galaxies (Moster *et al.*, 2010), reflecting different modes of formation, either at a fundamental level down to star forming regions, and/or at a global level reflecting the contribution from a supermassive black hole, from feedback associated to star formation, or even from the environment where galaxies live.

Star formation in galaxies seems to have two possible channels: “normal” star forming galaxies, such as our own Milky Way galaxy; and so-called starburst galaxies, where an intense rate of formation implies a much higher efficiency in the conversion of gas into stars. Fig. 1 (middle panel) shows that galaxies in the $1 < z < 3$ redshift window have a wide range of star formation efficiencies, from the

“quiescent” main sequence phase to intense starbursts. Various processes involving star formation, quenching and mergers have been invoked to explain the observed trends (Fig. 1, right panel). A very large number of papers have been devoted to this open problem, at the observational, theoretical and modelling levels. However, a definitive answer beyond simple sketches of the evolution is possible only with detailed spectroscopic information about the stellar content of galaxies over the peak of formation activity, i.e. $z \lesssim 3$. *Chronos* will obtain detailed formation histories over the range of stellar mass, redshift, and environment, required to decipher the mechanisms that control the efficiency of star formation.

... in a nutshell

- Complete sample of galaxies out to $z \sim 3$ down to $10^{10} M_\odot$ in stellar mass.
- Accurate assessment of environment over the most active period of galaxy formation, probing the interplay between dark matter and baryons.
- Detailed age, metallicity, abundance ratios, IMF: extragalactic archaeology.
- Understanding the mechanisms controlling the growth of galaxies: infall, outflows, AGN feedback, supernovae-driven winds.

Why do we need a new spectroscopic survey?

In the local Universe, SDSS provides detailed high quality spectroscopic information only out to a relatively modest apparent magnitude, and samples used for detailed spectroscopic analysis are often restricted to $z \lesssim 0.1$. In addition, the passband-shifting effect as we move into high

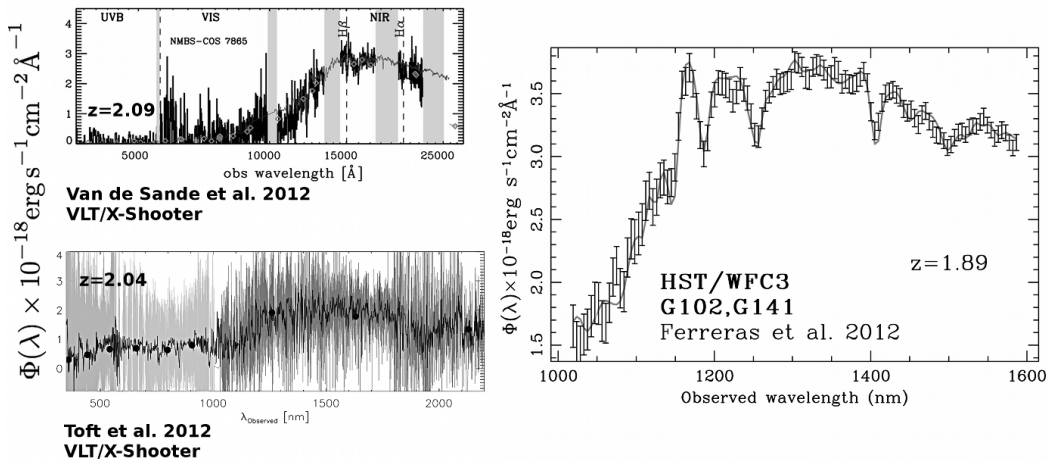


Figure 2: Comparison of NIR spectra from the ground (VLT/X-Shooter, left, comprising integration times of 5-7 hours) and from space (HST/WFC3 slitless grisms, with an integration of just over 1 hour). These galaxies are very massive, with an apparent magnitude $H_{AB} \sim 20$. *Chronos* will extract $\sim 1-2$ million spectra down to $H_{AB} \sim 25-26$.

redshift implies that the region around the 4000Å break – which is highly sensitive to the properties of the stellar populations – moves into the Near Infrared (NIR), so that future spectroscopic surveys in the optical region, such as MS-DESI (restricted to $\lambda < 1 \mu\text{m}$) will not be able to target galaxy formation at the peak of activity. In the NIR, ground-based observations are hampered by the high atmospheric background. Fig. 2 compares state of the art ground-based NIR spectroscopy of $z \sim 2$ galaxies taken by the X-Shooter instrument at ESO’s *Very Large Telescope* with a simple slitless grism spectrum taken by the WFC3 on board the *Hubble Space Telescope* at a similar redshift. The ground-based data was obtained at a higher spectral resolution, nevertheless, the difference in SNR is remarkable. Even though the field of view and spectral resolution of the *HST* data falls far below our target specifications, the figure illustrates that a 2.5m telescope in space is capable of superb deep NIR spectroscopy unrivalled from the ground. In addition, the restriction of ground-based observations to the allowed bands *J,H,K* introduce “redshift gaps” that will prevent a comprehensive study. Quoting Silk & Mamon (2012): “Ultimately, one needs a spectroscopic survey akin to SDSS at $z=1-2$ ”. However, *even with the large field of view provided by Subaru’s prime focus instruments (e.g. PFS), the quality required for a comprehensive analysis of the stellar populations of galaxies over the $z \sim 1-3$ range requires a space telescope.* Over a 5 year period, *Chronos* will deliver millions of high quality spectra plunging down to a flux level between 100 and 500 times lower than those shown in Fig. 2. In the future, observatories such as the *E-ELT* from the ground or *JWST* from space will be capable of achieving such low flux levels. However, the very small field of view covered by these facilities will make surveys over many square degrees unfeasible. *As a consequence, neither E-ELT nor JWST will be capable of investigating the large scale environment of high redshift galaxies. Chronos* will

be the only facility able to provide a large dataset of deep, high quality spectroscopic data in the NIR over large areas of the sky, required to properly assess the role of environment on the physical properties of galaxies and on their evolution. Neither broad-band nor medium-band photometric surveys such as DES, J-PAS or LSST can give enough “spectral resolution” to answer the key open questions of galaxy formation and evolution. Even at moderate resolution (e.g. ESA’s *Euclid* – and possibly NASA’s *WFIRST* – will provide $R \lesssim 600$ slitless grism spectroscopy, where the effective resolution is limited by the extent of the surface brightness profile of the galaxy), it will not be possible to obtain accurate constraints on the processes underlying the formation of stars in galaxies. Furthermore, as cosmology-orientated surveys, they are not designed to achieve high enough signal-to-noise ratio in the continuum for faint sources, a strict requirement in our mission. Nevertheless, for our purposes, *Euclid* is, rather, a valuable complement, as it will greatly help in the selection of targets for detailed spectroscopy with *Chronos*, providing in addition morphological information and photometry in several bands.

II.2 Probing galaxy formation through their stellar content

The redshift range of $z \sim 1-3$ is a fundamental epoch of galaxy formation for several reasons:

- (A) It is the peak of the cosmic star formation history (Hopkins & Beacom, 2006).
- (B) It is the peak of the AGN activity (Richards *et al.*, 2006).
- (C) It is the peak in the merger rate (Ryan *et al.*, 2008).
- (D) It is the epoch when hosting haloes of massive galaxies allows for cold accretion via cosmic streams (Dekel *et al.*, 2009).

Looking at the star formation history of galaxies today via moderately high resolution spectra reveals the integrated star formation history of these galaxies over all their progenitors (Thomas *et al.*, 2005; De la Rosa *et al.*, 2011). The hierarchical paradigm of structure formation predicts that the number of such progenitors can be quite significant (e.g., Khochfar & Silk, 2006). However, based on observational constraints at $z=0$, it is not possible to estimate the importance of the role of such progenitors and hence the role of merging. This is mainly due to the ‘cosmic conspiracy’ of the star formation main sequence, which, to first order, shows a linear relation between star formation rate and stellar mass of the galaxy (Daddi *et al.*, 2007). Thus, by knowing the star formation rate of a present-day galaxy at any higher redshift, it is not possible to determine whether it formed all its stars in one main progenitor or in many. The *only* viable option to observationally relate the star formation history and the mass assembly history involves deep spectroscopic observations, probing the underlying stellar populations during the peak of activity. A complete mass-limited sample will serve as an fundamental, unbiased benchmark to relate galaxies at different redshifts with their merging histories.

Chronos will provide a definitive statement on the formation timescale of galaxies with respect to morphology, mass and environment. It will also deliver information about the velocity dispersion and chemical enrichment of the populations. Such studies not only constrain but also motivate significant developments in numerical simulations in a cosmological context, to achieve a more consistent view of how galaxies form and evolve. For instance, the evidence that massive galaxies are old and enhanced in Mg over Fe (e.g., Renzini, 2006, and references therein) points towards an early and rapid formation, thus constraining the timescales in which haloes in regions of the Universe that are destined to form a cluster collapse (e.g., De Lucia *et al.*, 2006). A powerful test of these models is to study differences in the stellar content of galaxies in different environments. However, the evolutionary trends of stellar populations can be hidden due to the age-metallicity degeneracy, which not only affects the colours but also to a great extent the absorption line-strength indices of the old stellar populations (e.g., Worthey, 1994), if there is a relation between the age and the metallicity of the galaxies (e.g., Ferreras *et al.*, 1999). Much progress has been made during the last decade to lift this degeneracy, however, the chief aspect of this spectroscopic survey is that the targeted redshift interval represents a range in lookback time that resolves the “age axis” directly. Furthermore, studying the galaxies when they were younger allows to derive much more accurate ages as, in this regime, the spectral indicators have much larger variations for smaller changes in the mean age (Jørgensen *et al.*, 2013).

Constraining the characteristic timescales for the formation of the bulk of the stellar populations has been a major

endeavour. This is performed through the study of the chemical composition of galaxies derived from their spectra. As different elements are released to the interstellar medium by stars of different masses and, therefore, over different timescales, stellar and gas abundance ratios (once suitably calibrated) provide potential cosmic ‘clocks’ capable of eliciting the timescale of star formation within a galaxy. It is important to understand how non-solar abundance-patterns might affect the main conclusions derived from the stellar population analysis. These timescales can be fine tuned if, apart from [Mg/Fe], other abundance ratios, such as [CN/Fe], are included in this analysis (e.g., Carretero *et al.*, 2004). However, the different behaviour of elements released by massive supernovae (e.g., Woosley *et al.*, 2002) remain unclear, among other reasons, because these studies are still in their infancy. The dearth of quality spectroscopic observational datasets over a wide range of cosmic time explains the deficiencies of our understanding on the distribution of chemical elements in galaxies.

Efficiency of star formation

The efficiency of converting baryons into stars within given dark matter haloes is of prime interest. Theoretical predictions of LCDM-based models suggest a state of self-regulation in which the star formation rate is controlled by the growth rate of dark matter haloes (see, e.g., Bower *et al.*, 2006; Bouché *et al.*, 2010; Bower *et al.*, 2012; Guo *et al.*, 2013). The unprecedented sample of galaxies that *Chronos* will provide over the $z\sim 1-3$ range will allow us to construct high precision correlation functions for the galaxy population, including detailed information about their star formation histories, relating galaxy growth with the underlying distribution of dark matter structure. In this way, it will be possible to link measured star formation histories to theoretically predicted growth rates of dark matter haloes. It has been shown in studies at low redshift, that by only using abundance matching techniques it is not possible to obtain robust constraints on the galaxy halo occupation function (Neistein *et al.*, 2011).

Galaxy Formation and the Initial Mass Function

One of the most fundamental properties of star formation, the stellar Initial Mass Function (IMF), which describes the mass distribution of stars at birth, is assumed to be universal and constant with cosmic time. Recently, it has been argued that the stellar initial mass function may not be universal; differences have been hinted in the most massive galaxies at $z\sim 0$ (van Dokkum & Conroy, 2010; Cappellari *et al.*, 2012). A combination of a large, high-quality spectroscopic dataset from SDSS and detailed population synthesis models (Vazdekis *et al.*, 2012) enabled the confirmation of a systematic trend with velocity dispersion (Ferrerias *et al.*, 2013; La Barbera *et al.*, 2013). Such non-universality reflects fundamental differences in the mode of star formation with respect to galaxy mass (Hopkins,

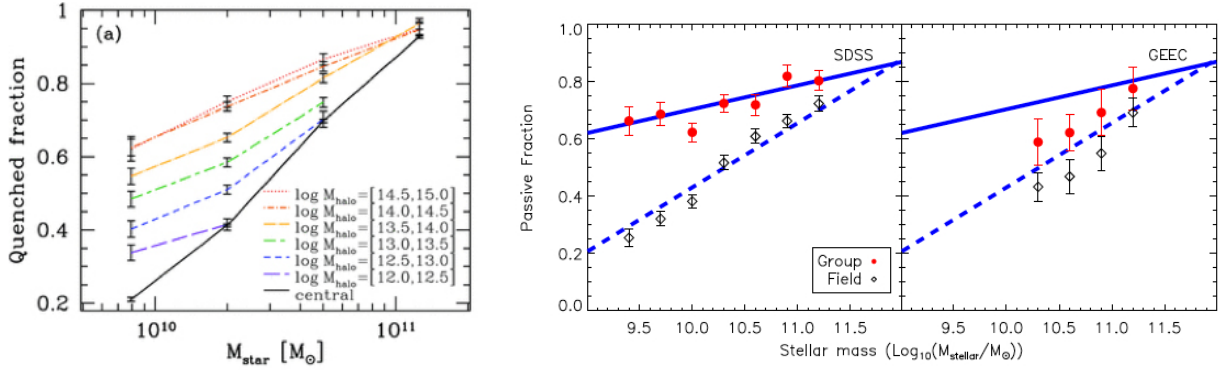


Figure 3: **Left:** The fraction of quenched galaxies (whose specific star formation rate is lower than 10^{-11} yr^{-1}) as a function of their stellar mass M_* , for galaxies residing in environments of different content of dark matter (M_{halo}). The solid line shows the variation of the fraction of quenched central galaxies (the most massive galaxy within each environment) in M_* (from Wetzel *et al.*, 2012). **Right:** The fraction of quenched galaxies as a function of their stellar mass in galaxy groups and in the field, as measured at $z \simeq 0$ in the SDSS survey and at $z \simeq 0.4$ in the GEEC survey (from McGee *et al.*, 2011).

2012), that need to be addressed in ab initio simulations of star formation (e.g. Bate *et al.*, 2003). Furthermore, recent theoretical developments suggest that the IMF shape and mass-cutoffs might depend on the star formation rate (Weidner *et al.*, 2011). However, the imprints of a varying IMF on spectra might be coupled to a variation of the abundance ratio of certain chemical species (Conroy & van Dokkum, 2012). Future population synthesis models (see II.6) along with high quality spectroscopic data of galaxies probing a wide range of cosmic time will allow us to disentangle these effects. With *Chronos*, it will be possible to probe the evolution of the IMF during the most important epoch of star formation, spanning a range of mass, velocity dispersion and metallicity. This issue is fundamental for an accurate assessment of the cosmic star formation history – which depends on the assumptions made for the underlying stellar populations. Moreover, derived star formation histories may have to be revised depending on these results, as a systematic change in the IMF can affect the model predictions relating the distribution of stellar ages and metallicities. We emphasize that such studies require high quality NIR spectroscopic data of very faint sources, such as those that *Chronos* will provide, beyond the capabilities of any spectroscopic survey in the coming decades.

II.3 The ecology of galaxies

In addition to the intrinsic mechanisms described above, the environment where galaxies live plays a fundamental role in shaping their evolution, as it is capable of quenching their star formation by removing their hot and cold gas reservoirs and to literally disrupt them by removing their stars. From the observed properties of galaxies at $z \simeq 0$ we have collected a large body of evidence for the occurrence of such environmental processes, but the determination of their timescales and amplitudes remains at a qualitative level. We have not yet established in a quantitative way

how these parameters depend on environment and redshift, i.e. on the assembly history of a galaxy cluster or galaxy group, through cosmic time.

The unprecedented statistical power of SDSS, in terms of the photometric and spectroscopic properties of galaxies measured at optical wavelengths, has allowed us to describe the behaviour of the star formation activity of galaxies across many orders of magnitude with respect to their stellar mass and environment at $z \simeq 0$. We know that the population of quenched galaxies – not forming new stars any longer – increases with their stellar mass for a given kind of environment, and with environment size (from small galaxy groups to large clusters) at fixed stellar mass (see Fig. 3, left; Weinmann *et al.*, 2006; van den Bosch *et al.*, 2008; Pasquali *et al.*, 2009; Wetzel *et al.*, 2012).

Galaxies become increasingly older (in terms of the mean age of their stars) as their environment becomes more massive (from galaxy groups to clusters), suggesting that galaxies in today’s clusters were accreted at earlier times (i.e. at a higher redshift of infall) than galaxies in today’s groups and had their star formation activity suppressed for longer times (Pasquali *et al.*, 2010). Most likely the quenching of their star formation activity happened while these galaxies were still living in smaller groups, which merged at later times with bigger structures like galaxy clusters.

Unfortunately, observations of $z \simeq 0$ galaxies can not constrain their redshifts of infall, or the time when they were subjected to environmental effects for the first time. Both *Euclid* and *Chronos* will trace the assembly history of environments with cosmic time and provide us with a direct measurement of the redshift of infall of galaxies as a function of their stellar mass. In addition, the lensing information from *Euclid* will be combined with the spectroscopic information produced by *Chronos* to probe the dependence of the star formation histories on the dark matter halos. However, while *Euclid* will only trace the assembly of the

very massive end, with a significant bias towards star-forming galaxies, *Chronos* will extend the study to smaller masses, including old populations, and therefore, avoiding the selection bias of the *Euclid* sample. A comparison of the $z \simeq 0$ data with the predictions of semi-analytic models of galaxy evolution indicates that galaxies should quench their star formation over a few billion years; this is the only available and indirect estimate of the timescale for environmental quenching of star formation and it is unclear how much it depends on environment and whether it has changed with redshift. When and in which environments did the quenching of the star formation activity of galaxies start? How fast did it proceed? The quantitative and direct answers to these questions come from the measurements of star formation rates, star formation histories and chemical enrichment of galaxies of different stellar mass, in different environments at different epochs, from $z \sim 1-3$ to $z=0$. Only these observables provide a direct estimate of the typical timescales of star formation in galaxies and hence a model-independent estimate of the timescales with which different environments succeeded in quenching their member galaxies of different stellar mass, and gave rise to the present-day galaxy populations.

With increasing redshift such measurements move to infrared wavelengths and become challenging even for modern ground-based telescopes. The intervening Earth atmosphere offers us only a partial disclosure of galaxies properties at $z > 0.5$; we can mostly measure emission lines (hence star formation rates), while absorption lines (age and metallicity indicators) become less and less accessible. From the data collected so far on galaxies at $0.3 < z < 0.8$, we know that the fraction of quenched galaxies is larger in galaxy groups than in the field, but definitively lower than the fraction of quenched galaxies in groups at $z \simeq 0$ (see Fig. 3, right; Wilman *et al.*, 2005; McGee *et al.*, 2011). At intermediate redshifts, the fraction of star forming galaxies decreases from 70-100% in the field to 20-10% in the more massive galaxy clusters (Poggianti *et al.*, 2006). Nevertheless, in terms of their star formation rates, galaxies in groups are not significantly different from those in the field; only star forming galaxies in clusters exhibit star formation rates a factor of 2 lower than in the field at fixed stellar mass (Poggianti *et al.*, 2006; Vulcani *et al.*, 2010; McGee *et al.*, 2011).

In the highest redshift range probed for environment at present, $0.8 < z < 1$, the more massive galaxy groups and clusters are populated mostly by quenched galaxies along with a 30% fraction in post-starburst galaxies (i.e. with a recently truncated star formation activity; Balogh *et al.*, 2011). The fraction of post-starburst galaxies is a factor of 3 times higher in clusters than in the field. Cluster and field galaxies are instead very similar in terms of the strength of their star formation activity and the amount by which their star formation has been quenched. These results have led Muzzin *et al.* (2012) to conjecture that either the quenching

of star formation due to the secular evolution of galaxies dominates over the quenching induced by galaxy environment, or both mechanisms occur together with the same timescale. Which timescale? We do not currently know. In order to make further progress, we require a facility such as *Chronos* to observe a complete stellar-mass limited sample of environments at $z \gtrsim 1$, and to measure the star formation histories of their galaxies with an unprecedented accuracy, thus providing the fading timescales of star formation of galaxies of different stellar mass inhabiting different environments. This is not simply an incremental step in our knowledge of environment-driven galaxy evolution. This is the *fundamental quantitative change* from the simple head-count of quenched or star forming galaxies to the measurement of physical properties of galaxies in environments at $z \gtrsim 1$, during the peak of galaxy formation activity. Such a step makes it possible to compare for the first time the same physical properties of galaxies at fixed stellar mass in different environments between $z=0$ and $z \gtrsim 1$, and to firmly quantify the extent to which environment regulates and modifies galaxy evolution across cosmic time.

II.4 Revealing the stellar population content of $z \sim 1-3$ galaxies

Understanding the nebular and stellar population properties of high redshift galaxies is an essential step towards a self-consistent picture of galaxy formation and evolution. The study of strong emission lines in the spectra of galaxies at $z \gtrsim 1$ has recently led to important results on the gas-phase properties, like the fact that metallicity exhibits a sharp transition towards subsolar values at $z \gtrsim 2.5$ (e.g., Möller *et al.*, 2013), and gas-rich disks are more dispersion dominated than in the nearby Universe (e.g., Förster-Schreiber *et al.*, 2011). Both results point to a major role of the accretion of unprocessed gas during the assembly of galaxies. In stark contrast, little is known about the stellar population content (i.e. the overall star formation history, metallicity, and IMF) of galaxies at $z > 1$.

Extracting star formation histories from spectra: An example

Fig. 4 (left) illustrates the reason for this impasse, that will render problematic our understanding of galaxy formation and evolution in the coming two decades. The upper panel plots a synthetic model spectrum, resembling the progenitor of a nearby early-type galaxy with mass $3 \times 10^{10} M_{\odot}$, as seen at $z=2$ (grey spectrum). The bottom panel shows the typical emission spectrum from the night sky (blue) as well as telluric absorption (grey). Such a high background – several orders of magnitude higher than the signal – makes the spectrum intrinsically inaccessible from a ground-based observatory, regardless of its photon collecting power (see also Fig. 2). The synthetic spectrum of Fig. 4 is obtained as

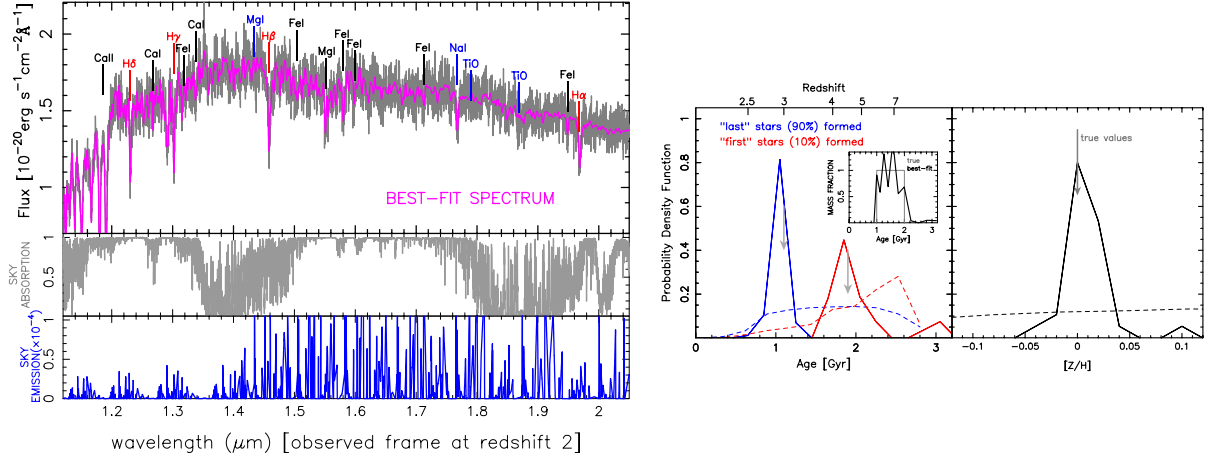


Figure 4: **Left-Top:** Synthetic spectrum resembling the progenitor of a nearby early-type galaxy, with a stellar mass of $3 \times 10^{10} M_{\odot}$, at $z \sim 2$ with a SNR of 20 per resolution element (grey). The best-fit model – obtained by direct spectral fitting – is overplotted in magenta. Some spectral features, sensitive to the star formation history (red), metallicity/abundances ratios (black), and IMF (blue) are included. **Left-Bottom:** sky emission (blue) and telluric absorption (grey), make the target spectrum very challenging from the ground. **Right:** Constraints on the timescales of star formation (left) and metallicity (right), derived from the spectrum on the left. The vertical grey arrows mark the input values. On the left, marginalized probability distribution functions (PDF) of the first (blue) and last (red) time of star formation (corresponding to 10% and 90% of total stellar stars formed). The inset shows the “true” star formation history of the system (grey histogram), and one typical best-fitting estimate (black curve). Note that a deep photometric survey cannot constrain the SFH or the metallicity in detail (dashed lines in both panels)

a linear combination of simple stellar population models from the MILES synthetic library (Vazdekis *et al.*, 2010), assuming that the galaxy starts forming stars at $z \approx 5$ (corresponding to an age of ~ 2 Gyr at $z = 2$), at a constant rate, with solar metallicity and a Kroupa-like IMF, down to $z \sim 3$ (Age ~ 1 Gyr), when star formation is suddenly quenched (because of, e.g., internal and/or environmental processes). The SNR of the spectrum (~ 20 , per resolution bin at $R=1500$) corresponds to a deep exposure, as planned for the *Chronos* ultra-deep survey (see Sec. V). Notice the strong Balmer lines in the spectrum (e.g. H β and H δ), that reflect the recent (~ 1 Gyr) quenching of star formation – a fact only recently observed at $z \sim 1.5$ (Bezanson *et al.*, 2013; Ferreras *et al.*, 2013), and eventually attributable to the presence of an AGN through suitable diagnostic lines that, at $z \gtrsim 1$, are hard to observe from the ground (e.g. H α and the companion [NII] line). A survey like *Chronos* is therefore required for the redshift range corresponding to the peak of galaxy formation activity.

Several absorption lines can be measured in the spectrum, most being sensitive to total metallicity and to the chemical abundances of individual elements (e.g. Mg, Si, Ti, Ca, Na), and some of them also to the fraction of dwarf-to-giant stars in the stellar IMF (e.g. the TiO features, see blue hatched regions). While the measurement of (total) metallicity and, to a lesser degree, that of $[\alpha/\text{Fe}]$ abundance ratio are a common practice in the case of low-redshift galaxies (e.g., Gallazzi *et al.*, 2005; Thomas, Maraston, Johansson, 2011), abundance estimates of single chemical species at low- z has become feasible only recently (e.g., Johansson,

Thomas, Maraston, 2012; Conroy *et al.*, 2013), thanks to the rapid development of stellar population models and spectral fitting techniques. During the next two decades we will develop superb stellar population models and software tools, to constrain also the star formation histories, abundance patterns, and the stellar IMF in high redshift galaxies, provided that their spectra will become accessible. Estimating metallicity and abundance ratios for galaxies at $z > 1$ would therefore give us crucial insights into the chemical enrichment history of galaxies (infall versus outflows of cold gas, and preferential loss of metals from supernovae-driven winds), nucleosynthesis yields, and the time-delay distributions of different types of SNe (e.g. Type Ia relative to core-collapse, driving the $[\alpha/\text{Fe}]$ of a stellar population at different epochs), as absorption features at high redshift would reflect the abundance of different elements by the time and immediately after they are synthesized in a galaxy.

During the next decade, direct fitting of stellar population models to data will likely become the “standard” tool to optimally extract the spectral information, compared to other well consolidated approaches like the analysis of line strengths (e.g. Lick-system indices). The magenta curve in the top panel of Fig. 4 (left) shows the result of fitting the ultra-deep-survey-like synthetic spectrum with a linear combination of 50 simple stellar populations, with different ages and metallicities. Notice that internal reddening – certainly important at high redshift – is set to be zero when synthesizing the spectrum, while it is included as a free parameter in the fitting procedure. The superb quality of

the fit will be typical for data of the quality we envisage for *Chronos*, with flux calibration accuracy better than a few percent.

Fig. 4 (right) illustrates the possibility of constraining timescales and metallicity for targets in the ultra-deep survey. One hundred noise realizations of the above mock spectrum are fitted as shown in Fig. 4, deriving from each best-fitting mixture some relevant, illustrative, parameters, i.e. the first and last epochs of star formation as well as the average metallicity. The first and last epochs are defined by the times when the system formed 10% and 90% of its stellar mass, respectively. Hence, NIR spectra with the given combination of SNR and resolution allows us to constrain sufficiently the formation timescales of a stellar population at redshifts corresponding to the peak of formation activity, as well as its total metal content (at less than 10%).

Velocity dispersion (not shown in the plot) can also be constrained with a <10% accuracy. Notice that the last epoch of star formation is connected to the quenching mechanism (e.g. AGN and/or environment), while the first epoch is ultimately driven by the initial conditions of density perturbations, along with other subtle physics (like reionization preventing star formation in small halos) illustrating the possibility to finally understand galaxy evolution in a full cosmological framework. In comparison, deep photometric surveys will not be able to compete on this front: the dashed lines in Fig. 4 (right) show the constraining power when only using broadband photometry, simulating data for the same galaxy, at $H_{AB}=25$, from a survey 1 mag deeper than the *Euclid* wide survey, and using a wide photometric coverage: $rizYJH + K$.

II.5 Towards the first galaxies

Chronos will be designed primarily in order to obtain a complete mass-limited sample of galaxies down to $\sim 10^{10}M_{\odot}$ over the $1 \lesssim z \lesssim 3$ redshift interval. In addition, this redshift range allows us to observe the rest-frame spectral window around the 4000Å region, a highly sensitive area to the age distribution of stars and their chemical composition. Beyond this, though, the capabilities of the instrumentation also opens up the $3 \lesssim z \lesssim 6$ redshift range. Although at those redshifts it will not be possible to observe mass-limited samples, *Chronos* will obtain SFRs from the NUV emission, which – complemented with stellar mass estimates from additional photometry from *Euclid* and future ground-based NIR photometric surveys will give a snapshot of the evolution of the efficiency of star formation between the first phases of galaxy formation at $z \gtrsim 6$ (the topic of the next section), and the epoch at the peak of activity (this section), acting as a bridge between these two fundamental stages of cosmic evolution. In addition, rest-frame NUV spectral features such as Mg_{UV} (Daddi *et al.*, 2005) will help characterize the properties of the stellar populations, although with a significantly lower

precision with respect to the $z \lesssim 3$ sample.

II.6 Population Synthesis in 2030

The most common methodology for deriving relevant stellar population parameters from the integrated light of galaxies consists in confronting observational data to predictions from stellar population synthesis models (Tinsley, 1980). However this approach is hampered by various fundamental degeneracies such as that between the age and the metallicity (Worthey, 1994). There are also other limitations that entangle derivations of burst-age and burst-strength (Leonardi & Rose, 1996) or effects from the IMF (Vazdekis *et al.*, 2010). Such degeneracies are commonly tackled with targeted spectral indices, direct spectral fitting, or a combination of both. However, as the quality of these models rely on the employed ingredients, great efforts are being put to develop stellar models and spectral libraries. This goal is being achieved in part by means of new stellar evolutionary calculations, with updated input physics, which might eventually include Helium and atomic diffusion, and higher mass/metallicity/age resolution (Pietrinferni *et al.*, 2004). Stellar libraries at moderately high spectral resolution with varying abundance ratios, either theoretical (Coelho *et al.*, 2005) or empirical (Milone *et al.*, 2011) as well as theoretical stellar evolutionary tracks with varying element mixtures (Pietrinferni *et al.*, 2006) are being developed. These libraries will lead to new generations of stellar population synthesis models that are better suited to estimate the observed abundance patterns, including the measurement of *individual* abundance ratios, opening the field of extragalactic archæology. This information puts the mass-metallicity relation “under the microscope”, allowing us to quantify in detail the various aspects of galactic chemical enrichment, including the effect of infall and outflows, and its connection with environment (Kawata & Mulchaey, 2008); or the dispersion of metals into the intergalactic medium (Pontzen *et al.*, 2008). In addition, developments in stellar libraries in the NUV (e.g., Koleva & Vazdekis, 2012) will optimise the methodology to extract information from the $z \gtrsim 3$ sample (see II.5).

The advent of models predicting galaxy spectra at moderately high resolution (e.g., Bruzual & Charlot, 2003; Vazdekis *et al.*, 2010) has opened the possibility of establishing robust constraints on the star formation histories, via a variety of full spectrum-fitting methods (e.g., Koleva *et al.*, 2008). There is a growing body of publications based on this approach as it allows us not only to attempt to estimate the star formation history (see II.4) but also to interpret better the results based on line-strength indices, which are more biased towards recent bursts and therefore hide the contributions weighted by mass. These estimates are particularly relevant for assessing the various mechanisms proposed for the assembly of galaxies and the role

of environment.

II.7 Synergy with *Herschel*

The synergies with *Euclid* are obvious, and throughout this white paper there are abundant references to the use of the *Euclid* surveys to aid in the target selection, analysis and interpretation of the data. We devote this subsection to another of ESA’s flagship missions: *Herschel* has provided, for the first time, efficient imaging of large areas of the sky in the far-IR window, from 70 to 500 μm . In particular, the *Herschel* Multi-tiered Extra-galactic Survey (HerMES, Oliver *et al.*, 2010) – the largest project on *Herschel* at 900 hrs – mapped over 70 deg^2 , tracing dust-enshrouded star-formation sources during the peak of galaxy mass as-

sembly. *Chronos* will be essential to take full advantage of the legacy of the *Herschel* surveys providing unique spectroscopic follow-up. Indeed, a detection in the FIR implies large amounts of dust emission, i.e. reprocessed light from the UV stellar emission. As a result the optical/near-IR SEDs are often very red and a large fraction of luminous *Herschel* galaxies are very faint or undetected in the optical bands, requiring deep NIR spectroscopy for their redshift measurements. However, over 90% of the 250 μm -detected sources have a counterpart at $K_{\text{AB}} < 24$. The *Chronos* surveys are thus optimally designed to exploit in full the investment of ESA in HerMES, providing redshifts, dynamical masses, stellar population properties, local environment and clustering for essentially all of the sources detected in the HerMES survey.

III. COSMIC REIONIZATION & GALAXY/BLACK-HOLE FORMATION

III.1 Introduction

Cosmic reionization is a landmark event in the history of the Universe. It marks the end of the “Dark Ages”, when the first stars and galaxies formed, and when the intergalactic gas was heated to tens of thousands of degrees Kelvin from much lower temperatures. This global transition, during the first billion years of cosmic history, had far-reaching effects on the formation of early cosmological structures and left deep impressions on subsequent galaxy and star formation, some of which persist to the present day.

The study of this epoch is thus a key frontier in completing our understanding of cosmic history, and is currently at the forefront of astrophysical research (e.g. Robertson *et al.*, 2013). Nevertheless, despite the considerable recent progress in both observations and theory (e.g. see recent reviews by Dunlop 2013 and Loeb 2013) all that is really established about this crucial era is that Hydrogen reionization was completed by redshift $z \simeq 6$ (as evidenced by high-redshift quasar spectra; Fan *et al.* 2006) and probably commenced around $z \sim 15$ (as suggested by the latest WMAP9 microwave polarisation measurements, which favour a ‘mean’ redshift of reionization of 10.3 ± 1.1 ; Hinshaw *et al.* 2013). However, within these bounds the reionization history is essentially unknown, and new data are required to construct a consistent picture of reionization and early galaxy formation/growth.

Unsurprisingly, therefore, understanding reionization is one of the key science goals for a number of current and near-future large observational projects. In particular, it is a key science driver for the new generation of major low-frequency radio projects (e.g. LOFAR, MWA and SKA) which aim to map out the cosmic evolution of the *neutral*

atomic Hydrogen via 21-cm emission and absorption. However, such radio surveys cannot tell us about the sources of the ionizing flux, and in any case radio observations at these high redshifts are overwhelmingly difficult, due to the faintness of the emission and the very strong foregrounds. It is thus essential that radio surveys of the neutral gas are complemented by near-infrared surveys which can both map out the growth of ionized gas, and provide a complete census of the ionizing sources. A genuinely multi-wavelength approach is required, and cross-correlations between different types of observations will be necessary both to ascertain that the detected signals are genuine signatures of reionization, and to obtain a more complete understanding of the reionization process.

It has thus become increasingly clear that a *wide-area, sensitive, spectroscopic* near-infrared survey of the $z=6-12$ Universe is required to obtain a proper understanding of the reionization process and early galaxy and black-hole formation. Such a survey cannot be undertaken from the ground, nor with *JWST* (inadequate field-of-view), or *Euclid* (inadequate spectroscopic sensitivity). Only a mission such as *Chronos* can undertake such a survey and simultaneously address the three, key, interrelated science goals which we summarize below.

... in a nutshell

- Charting the progress of reionization through the clustering of Ly- α galaxies.
- Determining the source of reionization.
- Studying the emergence of the first galaxies over cosmologically representative volumes.

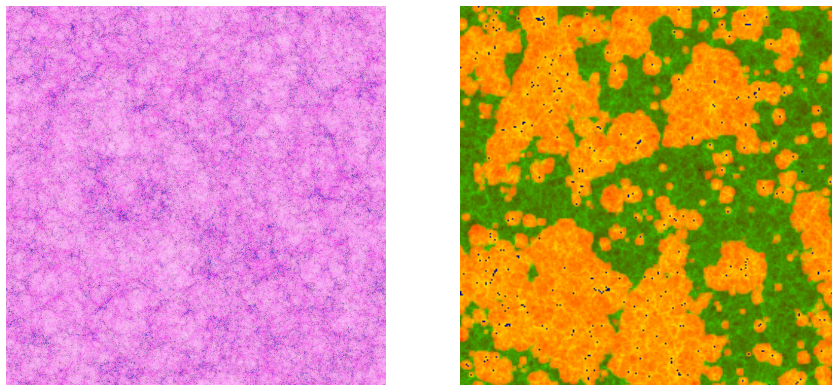


Figure 5: **Left** Early structure formation in Λ CDM (at $z = 6$) from an N -body simulation with 5488^3 (165 billion) particles and a volume $425 \text{ h}^{-1} \text{ Mpc}^3$. Shown are the dark-matter density (pink) and halos (blue). This synthetic image corresponds to 3.5×3.5 degrees on the sky. **Right:** The geometry of the epoch of reionization, as illustrated by a slice through a $(165 \text{ Mpc})^3$ simulation volume at $z = 9$. Shown are the density (green/yellow), ionized fraction (red/orange), and ionizing sources (dark dots) (Iliev *et al.*, 2012). The necessity of a deep, near-infrared spectroscopic survey covering many square degrees is clear.

III.2 The clustering of Lyman- α emitters as a probe of reionization

Cosmological simulations of the reionization process predict that the highly-clustered, high-redshift sources of Lyman-continuum photons will lead to an inhomogeneous distribution of ionized regions; the reionization process is expected to proceed inside-out, starting from the high-density peaks where the galaxies form. Thus, as demonstrated by the state-of-the-art simulations shown in Fig. 5, reionization is predicted to be highly patchy in nature. This prediction is already gaining observational support from the latest large-area surveys for Lyman- α emitters at $z \simeq 6.5$, where it has been found that, depending on luminosity, their number density varies by a factor of 2 – 10 between different $\simeq 1/4 \text{ deg}^2$ fields (Ouchi *et al.*, 2010; Nakamura *et al.*, 2011). It is thus clear that surveys over many square degrees are required to gain a representative view of the Universe at $z > 6$. Crucially, with such a survey, the differential evolution and clustering of Lyman-break galaxies and Lyman- α emitting galaxies can be properly measured for the first time, offering a key signature of the reionization process.

As has been well-demonstrated over recent years, galaxies at high-redshift can be very effectively selected on the basis of *either* their redshifted Lyman break (the sudden drop in emission from an otherwise blue galaxy, due to inter-galactic absorption at wavelengths $\lambda_{rest} < 1216 \text{ \AA}$), or their redshifted Lyman- α emission. The former class of objects are termed Lyman-Break Galaxies (LBGs) while the latter are termed Lyman- α Emitters (LAEs). In principle, LAEs are simply the subset of those LBGs which display detectable Lyman- α emission, but the current sensitivity limitations of broad-band near-infrared imaging over large areas has meant that narrow-band imaging has been successfully used to yield samples of lower-mass galaxies which are not usually identified as LBGs (e.g., Ono *et*

al., 2010). Nevertheless, as demonstrated by spectroscopic follow-up of complete samples of bright LBGs (e.g., Stark *et al.*, 2010; Vanzella *et al.*, 2011; Schenker *et al.*, 2012), the fraction of LBGs which are LAEs as a function of redshift, mass, and environment is a potentially very powerful diagnostic of both the nature of the first galaxies, and the physical process of reionization.

With the unique combination of deep, wide-area near-infrared imaging, provided by surveys such as *Euclid*, and deep, complete follow-up near-infrared spectroscopy, made possible with *Chronos*, we now propose to fully exploit the enormous potential of this approach. The essential idea of using *Chronos* to constrain reionization is as follows: while the Lyman- α luminosity of LAEs is affected both by the intrinsic galaxy properties, *and* by the H I content (and hence reionization), the luminosity of LBGs (which is measured in the continuum) depends only on the intrinsic galaxy properties. Thus, a deep, wide-area, complete survey for LBGs at $z \simeq 6$ –12 with accurate redshifts secured by *Chronos* will deliver a definitive measurement of the evolving luminosity function and clustering of the emerging young galaxy population, while the analysis of the follow-up spectroscopy will enable us to determine which LBGs reside in sufficiently large ionized bubbles for them to also be observed as LAEs. In order to prevent strong damping wing absorption of Ly α photons, a galaxy must carve out a bubble of radius R_I corresponding to a redshift difference with respect to the source of $\Delta z > 0.01$, or around 250 physical kpc at $z \simeq 8$. According to the most recent reionization history predictions from cosmological simulations, consistent with the various reionization constraints, the H I fraction at this redshift is around $\chi \approx 0.4 - 0.7$. It is easy to show that R_I for a typical galaxy with a star-formation rate of $\dot{M}_* = 1 M_\odot \text{ yr}^{-1}$ is of the same order or smaller, depending on poorly established values of the ionizing photon escape fraction. Thus, such galaxies will be only marginally detectable in the Ly α line if they are

isolated. In practice, some of these galaxies will be highly clustered and therefore will help each other in building a H II region which is large enough to clear the surrounding H I and make it transparent to Ly α photons.

This argument emphasizes the importance of clustering studies of LAEs, for which *Chronos* is optimally designed. A key aim is to compute in great detail the two-point correlation function of LAEs and its redshift evolution. For the reasons outlined above, reionization is expected to increase the measured clustering of emitters and the angular features of the enhancement would be essentially impossible to attribute to anything other than reionization. In fact, under some scenarios, the apparent clustering of LAEs can be well in excess of the intrinsic clustering of halos in the concordance cosmology. Observing such enhanced clustering would confirm the prediction that the H II regions during reionization are large (McQuinn *et al.*, 2007).

As required to meet our primary science goals, the *Chronos* surveys will result in by far the largest and most representative catalogues of LBGs and LAEs ever assembled at $z > 6$. Detailed predictions for the number of LBGs as extrapolated from existing ground-based and *HST* imaging surveys are deferred to the next subsection. However, here we note that the line sensitivity of the 100 deg² spectroscopic survey will enable the identification of LAEs with a Ly α luminosity $\geq 10^{42.2}$ erg s⁻¹, while over the smaller, ultra-deep 10 deg² survey this line-luminosity limit will extend to $\geq 10^{41.6}$ erg s⁻¹. Crucially this will extend the Lyman- α detectability of LBG galaxies at $z \simeq 8$, with brightness $J \simeq 27$ (AB mag), down to “typical” equivalent widths of $\simeq 15 \text{ \AA}$ (Stark *et al.*, 2010; Vanzella *et al.*, 2011; Curtis-Lake *et al.*, 2012; Schenker *et al.*, 2012).

The total number of LAEs in the combined *Chronos* surveys will obviously depend on some of the key unknowns that *Chronos* is designed to measure, in particular the fraction of LBGs which display detectable Ly α emission as a function of redshift, mass and environment. However, if the observed LAE fraction of bright LBGs at $z \simeq 7$ is taken as a guide, the *Chronos* surveys will uncover $\sim 10,000$ LAEs at $z > 6.5$.

III.3 The emerging galaxy population at $z > 7$, and the supply of reionizing photons

Chronos will provide a detailed spectroscopic characterization of an unprecedentedly large sample of LBGs and LAEs. Crucially, as well as being assembled over representative cosmological volumes of the Universe at $z \simeq 6-12$, these samples will provide excellent sampling of the brighter end of the galaxy UV luminosity function at early epochs. As demonstrated by the most recent work on the galaxy luminosity function at $z \simeq 7-9$ (McLure *et al.*, 2013), an accurate determination of the faint-end slope of the luminosity function (crucial for understanding reionization) is in fact currently limited by uncertainty in L^* and ϕ^* .

Consequently, a large, robust, spectroscopically-confirmed sample of brighter LBGs over this crucial epoch is required to yield definitive measurements of the evolving luminosity functions of LBGs and LAEs.

Leaving aside the uncertainties in the numbers of LAEs discussed above, we can establish a reasonable expectation of the number of photometrically-selected LBGs which will be available for *Chronos* spectroscopic follow-up by the time of the mission. For example, scaling from existing *HST* and ground-based studies, the ‘Deep’ component of the *Euclid* survey (reaching $J \simeq 26$, $5-\sigma$ over $\simeq 40 \text{ deg}^2$), is expected to yield $\simeq 6000$ LBGs in the redshift range $6.5 < z < 7.5$ with $J < 26$ (selected as “Z-drops”), $\simeq 1200$ at $7.5 < z < 8.5$ (“Y-drops”), and several hundred at $z > 8.5$ (“J-drops”) (Bouwens *et al.*, 2010; Bowler *et al.*, 2012; McLure *et al.*, 2013).

Therefore, the planned spectroscopic follow-up over 10 deg^2 , will be able to target (at least) $\simeq 1500$ LBGs in the redshift range $6.5 < z < 7.5$, $\simeq 300$ in the redshift bin $7.5 < z < 8.5$, and an as yet to be determined number of candidate LBGs at $8.5 < z < 9.5$. The proposed depth and density of the *Chronos* near-infrared spectroscopy will allow detection of Ly α line emission from these galaxies down to a $5-\sigma$ flux limit 1×10^{-18} erg cm⁻²s⁻¹, enabling rejection of any low-redshift interlopers, determination of the LAE fraction down to EWs of $\simeq 10 \text{ \AA}$, and accurate spectroscopic redshifts for the LAE subset.

III.4 The contribution of AGN to reionization & the early growth of black holes

SDSS has revolutionised studies of quasars at the highest redshifts, and provided the first evidence that the epoch of reionization was coming to an end around $z \gtrsim 6$ (Becker *et al.*, 2001). As with the studies of galaxies discussed above, pushing to higher redshifts is impossible with optical surveys, regardless of depth, due to the fact that the Gunn-Peterson trough occupies all optical bands at $z > 6.5$. Therefore, to push these studies further in redshift needs deep wide-field surveys in the near-infrared.

The wide-area, ground-based VISTA near-infrared public surveys such as VIKING and the VISTA hemisphere survey are slowly beginning to uncover a few bright quasars at $z \simeq 7$ (e.g., Mortlock *et al.*, 2011), and it is to be expected that *Euclid* will be able to provide a good determination of the very bright end of the QSO luminosity function at $z > 6$. However, the shape of the QSO luminosity function at these redshifts can only be studied with detailed near-infrared spectroscopy over a significant survey area. This is the only direct way to properly determine the contribution of accreting black holes to the reionization of the Universe and constrain the density of black-holes within the first Gyr after the Big Bang; *Chronos*’s combination of depth and area provides the ideal way in which to measure the evolving luminosity function of quasars at $6.5 < z < 10$.

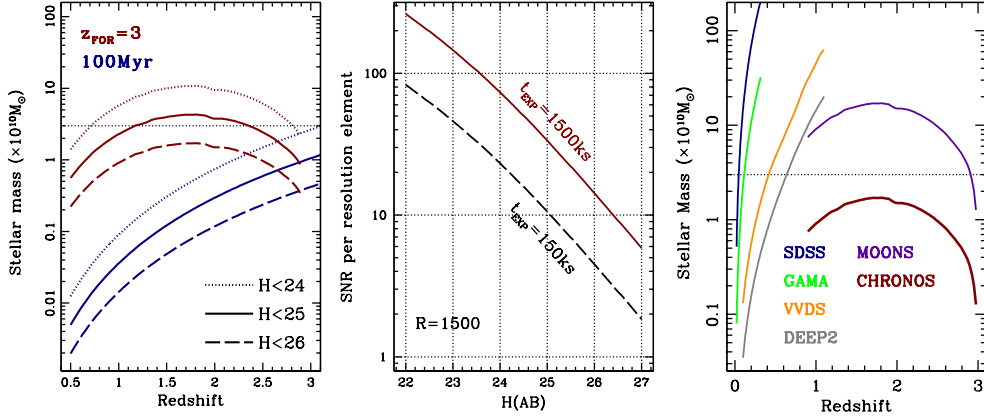


Figure 6: **Left:** Stellar mass versus redshift for three limiting-magnitude surveys, as labelled. The red lines correspond to old stellar populations, whereas the blue lines trace a more luminous, young population, corresponding to the typical age of a star forming galaxy. **Middle:** SNR per resolution element at $R \equiv \lambda/\Delta\lambda = 1500$ for a 2.5m (diameter) collecting area, 20% total efficiency, a zodiacal light (minimal) level of $H_{\text{AB}}=25$ and typical readout noise and dark current of cutting-edge NIR arrays ($\text{RN}=4e$, 0.01 e/s, respectively). We note that the SNR is estimated in the continuum, a much more stringent requirement than emission line estimates, typical of cosmology-orientated surveys. **Right:** Comparison of *Chronos* (wide survey) with a range of optical and NIR spectroscopic surveys with similar spectral resolution. The curves track the lower limit in stellar mass for an old population (i.e. the worst case scenario).

IV. ADDITIONAL SCIENCE CASES

Although this white paper deals with the core science driver of galaxy formation and evolution in the spectral window $1 \lesssim z \lesssim 12$, the legacy side of *Chronos* is immense, and additional science projects can be addressed. Among them, we list a few relevant cases below:

- i) Transients: the planned 5-year mission can accommodate the spectroscopic follow up of transients, most notably high redshift supernovae, allowing us not only to confirm the type of supernova, but spectroscopic features could be used to understand their properties and evolution, relevant to precision cosmology studies (Foley & Kasen, 2011).
- ii) Cosmology: *Chronos* will enable cosmological model testing beyond *Euclid*. As an example, measurements

of the velocity field, galaxy bias, and lensing potential simultaneously will enable a measurement of general single scalar-field models (e.g., Amendola *et al.*, 2012). The deep redshift range would also constrain early-dark energy models, complementing the *Euclid* cosmology objectives using techniques such as those used by Mandelbaum *et al.* (2012) in SDSS.

- iii) Brown dwarves: The *Chronos* survey could include a programme to explore cool T-dwarves out to a few hundred pc, allowing us to determine the scale height of this population. By targeting nearby star forming regions, we can probe the IMF down to Jupiter-size masses.

V. SURVEY REQUIREMENTS

The core requirement of the survey is the apparent magnitude limit to obtain a complete sample selected in stellar mass, with acceptable SNR per resolution element for the study of the underlying stellar populations. Any other criteria commonly approached in surveys (e.g. selection in luminosity or colour) will bias the sample. We use stellar population synthesis models (Bruzual & Charlot, 2003) to estimate the apparent magnitude with respect to

stellar mass and redshift for two extreme scenarios (Fig. 6, left panel). An old population (red lines) will lack the most massive and luminous stars, therefore appearing significantly fainter than a younger population with the same mass (blue lines). The age range used in the figure covers a conservative interval as obtained, e.g., from spectroscopic observations of the local Universe (Gallazzi *et al.*, 2005). The figure shows that at $H_{\text{AB}} \sim 26$, we will

obtain a complete sample out to $z \sim 3$ for galaxies with stellar mass around $1 - 2 \times 10^{10} M_{\odot}$. This is a *conservative* estimate, as observations suggest that there is a strong trend towards younger ages in low mass galaxies, with the characteristic star-forming galaxy appearing more massive at higher redshift (Pérez-González *et al.*, 2008). This trend implies that the majority of low-mass galaxies will be younger, allowing us to reach a completeness level – if we relax the constraint regarding old populations – at lower stellar masses, possibly around $10^9 M_{\odot}$, covering an unprecedented range of galaxy mass over the $z=1-3$ redshift window. The middle panel of Fig. 6 gives an estimate of the SNR per resolution element (at $R=1500$) achieved for two exposure times, as labelled. We envisage a two-tiered survey, comprising a wide-deep survey covering 100 deg^2 (corresponding to the dashed black line) and an ultra-deep survey with a 10 times longer integration over 10 deg^2 (solid red line). We emphasize here that a proper characterization of the stellar populations from spectroscopic data requires $\text{SNR} \gtrsim 5 - 10$. This figure assumes a low zodiacal and thermal background level, with a spatial resolution of 0.3 arcsec , and typical detector noise for the type of available arrays (e.g., Teledyne Hawaii 4RG). The rightmost panel of Fig. 6 compares the ability of *Chronos* to obtain a mass-limited sample out to a chosen redshift with recent or planned spectroscopic surveys at similar resolution. We note that neither *Euclid* nor *WFIRST* estimates are included in the figure, as their low-resolution, slitless grism spectra are not capable of achieving the goals of this white paper². *MOONS* is clearly the best option at present in the $z=1-3$ redshift range, however, the signal in the continuum will be weak unless very young populations are considered. Only *Chronos* can provide the collecting power and wide field of view to tackle in an unbiased way the analysis of galaxies at the peak of activity.

As regards to the required total areal coverage on the sky, we use as reference the SDSS, whose high quality spectroscopic data can be extended out to, at most, $z \lesssim 0.2$, covering a comoving volume of $5.5 \times 10^{-5} \text{ Gpc}^3$ per square degree. Over the proposed $z \sim 1-3$ range, we have 0.02 Gpc^3 per deg^2 . Hence, in order to probe the environment in detail comparable to the $\sim 10^4 \text{ deg}^2$ of SDSS/DR7 (Abazajian *et al.*, 2009), we need around 30 deg^2 . In addition, we expect environment to evolve significantly between the SDSS baseline and the goal of *Chronos*. We use a large cosmological simulation (Millennium, Springel *et al.*, 2005) to find an evolution in the number of a factor of $\sim 2-3$ for groups with halo mass $M_{\text{halo}} \gtrsim 10^{12} M_{\odot}$ at $z=0$. Therefore, the general survey should target around 100 deg^2 , putting this project outside of the reach of *JWST* or any of the extremely large telescopes on the ground. SDSS has also shown that datasets comprising ~ 1 million spectra are necessary to split the sample with respect to the many properties under consideration (velocity dispersion, luminosity, mass, environment, etc). Finally, an extrapolation of the Muzzin *et al.* (2013) data using a fit to a Schechter law gives a number density of 1.2×10^5 galaxies per square degree at the $H_{\text{AB}}=26$ level in the $z \sim 1-3$ range.

... in a nutshell

- At $H_{\text{AB}}=26$ we expect $\gtrsim 100,000$ galaxies per square degree at $z \sim 1-3$
- Completeness down to a stellar mass $\sim 10^{10} M_{\odot}$ ($z \lesssim 3$) for any population.
- Two surveys: 100 deg^2 and 10 deg^2 extending over the $z \gtrsim 1$ environments probed by SDSS at $z \lesssim 0.1$.
- The final dataset will comprise $\sim 1 - 2$ million high-quality spectra.

VI. STRAWMAN MISSION CONCEPT

VI.1 Mission Profile

As an infrared survey mission, the preferred orbit for *Chronos* is at the low background L2 point, with heritage from *Herschel* and *Planck* operations and, in the future, from *Gaia*, *JWST* and *Euclid*. An Ariane 5 ECA or ME launcher provides excellent payload margin with a limit to L2 in excess of 6.2 tonnes. The standard fairing has a length of 12.7 m and a diameter of 4.6 m which can easily accommodate the proposed *Chronos* spacecraft configuration; these dimensions would allow a full 2.5m diameter $f/1.2$ telescope to be deployed without any dynamic mechanisms.

Other launcher options could be considered, depending on launch date. Once L2 has been reached, the Δv requirements for orbit station and formation keeping are small ($< 75 \text{ m s}^{-1} \text{ year}^{-1}$).

The *Chronos* survey strategy will follow that adopted for the *Euclid* deep-field programme, with frequent revisits to the same field centres to build up S/N on faint targets, ameliorate the contamination effects in crowded fields, and provide useful cadence for serendipitous studies of high-redshift supernovae and gamma-ray bursts. The regular layout of the proposed *Chronos* focal plane will allow a simple tiling strategy to cover contiguous areas of the 100 deg^2

²Nevertheless, as a reference, the *Euclid* Definition Study Report states that at $z \geq 1.5$ only galaxies with a stellar mass $> 4 \times 10^{11} M_{\odot}$ will provide useable spectra for the analysis of the populations (Laureijs *et al.*, 2011).

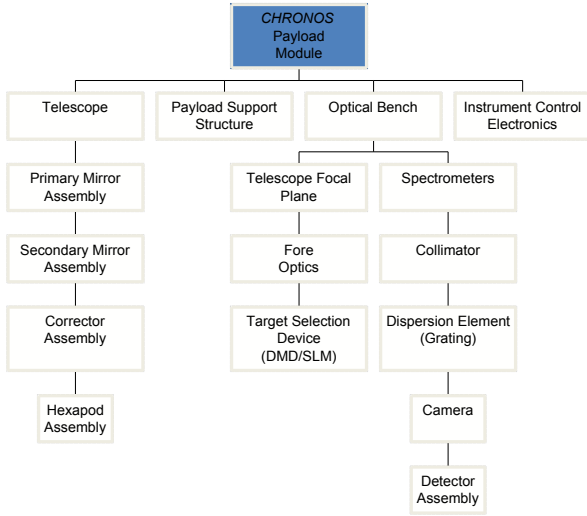


Figure 7: Subsystem breakdown of the payload module hardware.

(deep) and 10 deg^2 (ultra-deep) fields. For a 5 year mission, at a 70% operational efficiency, the draft survey plan calls for visiting one pointing per week (deep) or one pointing per 10 weeks (ultra-deep with 10x longer exposure). Assuming that *Chronos* targets 30% of the available sample at a multiplex of ~ 5000 , will require ~ 8 mask configurations per pointing, giving a total exposure time of 150 ksec for the deep survey and 1500 ksec for the ultra-deep survey. The final galaxy samples would thus comprise ~ 1.5 million (~ 150 thousand) high quality spectra in the deep (ultra-deep) surveys.

As a dedicated survey mission, the ground segment can be kept relatively simple. Target definition for the survey will come from the optical-infrared imaging in the *Euclid* deep fields or, as a fallback, from *LSST* and *VISTA* ground-based deep survey ($AB \sim 27.5$ optical and $AB \sim 24.5$ infrared respectively). Fast data analysis will be required only for the transient detection programme. The downstream data rate will be approximately 50 GB/day after compression (depending on the number of intermediate detector samples are transmitted); assuming a typical K-band rate of transfer to the ground of 50 Mbit/s, all of the data can be transferred to the ground with a contact time of 3 hours per 24 hours.

VI.2 Payload Description

The science requirements for *Chronos* drive the choice of a telescope with a 2.5m aperture and a 1 deg field-of-view feeding eight identical multi-object slit-based spectrometers with moderate spectral resolution and good background subtraction. Selection of the science targets for the spectrometers can be achieved by using a digital micromirror device (DMD) or other form of spatial light modulator. There is no scientific need to make *Chronos* into a multi-

Item	Payload Requirements
Telescope	
Primary mirror	2.5 metre diameter
Field of View	1.0 degree diameter
Image quality	EE(80) < 0.3 arcsec
Spectrometers	
Target multiplex	~ 5000 objects per pointing
Field of view	0.2 deg^2 (total, 8 spectrometers)
Spectral coverage	$0.9 \mu\text{m}$ to $1.8 \mu\text{m}$
Spectral resolution	$R \sim 1500$
Throughput	> 20% including detectors
Spacecraft	
Mass	< 4000 kg
Volume	
Diameter	3500 mm
Length	7000 mm

Table 1: Summary of the key performance requirements of the *Chronos* payload.

purpose observatory so the spectrometers have a single fixed resolving power ($R \sim 1500$). The DMD or spatial light modulator can be used to shut off the signal to the detectors, so no mechanisms are required. The payload module hardware breaks down into testable sub-systems as shown in Figure 7. The key performance parameters of the *Chronos* payload are shown in Table 1.

VI.2.1 Telescope Assembly

The 2.5-metre telescope could be a Korsch or Ritchey-Chrétien design for which a three-element field corrector which would give a field-of-view of 1 degree at $f/3$ to feed the eight spectrometers. Assuming a Ritchey-Chrétien design, this could be optimised to provide uniform image quality across the whole field with an image quality (EE80 ~ 0.3 arcsec) which is matched to the intrinsic size of galaxies at high redshift. Both the primary ($f/1.2$) and secondary ($f/3$) mirrors are hyperboloids. The secondary mirror (M2) is 0.9m in diameter and its mounting incorporates light sources for calibration of the spectrometer. While SiC will provide excellent performance if a 2.5m optical-quality mirror can be fabricated, lightweighted Zerodur would also be possible. The baseline design assumes that both M1 and M2 are fabricated from lightweighted Zerodur and are supported directly from the telescope support structure. A central light baffle incorporates the three fused silica corrector elements in the R-C design (two aspheric surfaces).

The telescope support structure is a SiC or CFRP space frame which supports all the hardware of the spacecraft, and under which is mounted the Instrument Optical Bench and the Instrument Service Module. The upper section of the telescope structure consists of a triangular frame, the corners of which act as structural nodes for the M1 back-

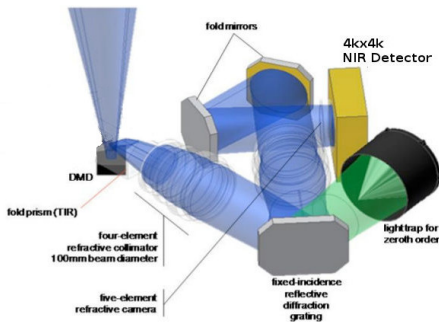


Figure 8: Close-up of a single spectrometer channel.

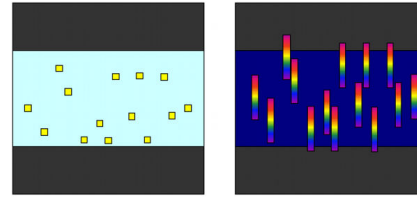


Figure 9: Schematic of multi object target selection using DMDs.

Phase A	30 Meuro
Phase B	200 Meuro
Phase C/D	600 Meuro
Launch	200 Meuro
Phase E/F	200 Meuro
Total	1230 Meuro

Table 2: *Chronos* lifecycle cost estimate, including national hardware contributions.

ing structure, the M2 hexapod and the instrument optical bench. The total length of the telescope is approximately 5 metres with a mass of 600 kg (excluding payload and service module).

VI.2.2 Spectrometer

At the heart of the *Chronos* concept are a set of eight multi-object spectrometers (Fig. 8), each capable of delivering complete samples of moderate resolution ($R \sim 1500$) near-infrared spectra for high redshift galaxies down to a magnitude limit of $H_{AB} \sim 26$ mag. To reach this faint limit requires ‘multi-slit’ spectroscopy with a target selection mechanism which is compatible with space operations. Our baseline approach is to use the Texas Instruments (TI) digital micro mirror devices (DMDs) which were originally proposed for the *SPACE* mission (Cimatti *et al.*, 2009). These are available in formats up to 2048×1080 pixels with a pitch of $13.68 \mu\text{m}$ and are currently at a technology readiness level of $\text{TRL} \sim 4$ (Zamkotsian *et al.*, 2010). Each of the individual micromirrors on the DMD can be switched into an ‘ON’ or ‘OFF’ position to define a *virtual* slit of 1.2×0.4 arcsec, centred on the target of interest, thus replicating the multislit masks used in ground-based spectroscopy of faint targets (Figure 9).

Simulations of the targeting efficiency of the DMD at the magnitude limit of the survey, indicate that each spectrometer can obtain the spectra for ~ 600 targets simultaneously, without spectral overlaps, giving a multiplex of ~ 4800 targets with eight spectrometers covering a total field of $\sim 0.2 \text{ deg}^2$.

To mitigate against qualification and availability of DMD devices in the timescale of an L2/L3 mission, a parallel technology development study should also be initiated early in the project to assess the technology readiness of other forms of target selection devices, including liquid crystal spatial light modulators and pupil beam steering devices.

The entrance apertures of the spectrometers will be positioned symmetrically within the telescope field of view to allow a simple step-and-stare operation to tile the sky contiguously. Each spectrograph will use refractive collimators

and cameras, feeding a $4\text{k} \times 4\text{k}$ HgCdTe infrared array. A 60 lines/mm grating is used to produce a Nyquist sampled spectrum covering the range $0.9\text{--}1.8 \mu\text{m}$.

VI.3 Operational Model

The *Chronos* operational model follows the usual lines of a survey-type project. The satellite will operate autonomously except for defined ground contact periods during which housekeeping and science telemetry will be downlinked, and the commands needed to control spacecraft and payload will be uploaded. The data rate is around 50 GB/day which is easily handled with current data-processing systems. A data model for the mission will be developed in collaboration with ESA. Based on the data model, an archive system will be built, enabling data archiving, data processing and distribution of all *Chronos* observations with appropriate levels of processing, including all the necessary ancillary information.

VI.4 Programmatics and Cost

Chronos is envisaged as a typical science mission with ESA having overall control, but with a major contribution from a consortium of European institutes in the form of the science payload and ground segment. The mission has been designed to ensure that technologies with space heritage or high TRL are used where possible. The DMDs are an exception to this, although good progress has already been made in developing these for space application for the original *SPACE/Euclid* mission concepts. We believe that this technology can be further developed in good time for the *Chronos* mission and will thus not be a schedule driver. An approximate cost per phase is shown in Table 2.

... in a nutshell

- 2.5m telescope, Korsch or Ritchey-Chrétien in SiC
- 8 spectrometers, $R=1500$, 4800 multiplex.
- 5 year mission at L2.
- Ariane 5 launcher.

REFERENCES

- Abazajian, K. N., *et al.*, 2009, *ApJS*, 182, 543
 Amendola, L., *et al.*, 2012, *Phys. Rev. D*, 85, 3008
 Balogh, M.L., *et al.*, 2011, *MNRAS*, 412, 2303
 Baldry, I. K., *et al.*, 2004, *ApJ*, 600, 681
 Bate, M. R., Bonnell, I. A., Bromm, V., 2003, *MNRAS*, 339, 577
 Becker, R., *et al.*, 2001, *AJ*, 122, 2850
 Bezanson, R., *et al.*, 2013, *ApJ*, 764, 8
 Bouché, N., *et al.* 2010, *ApJ*, 718, 1001
 Bouwens, R., *et al.*, 2010, *ApJ*, 709, 133
 Bower, R. G., *et al.*, 2006, *MNRAS*, 370, 645
 Bower, R. G., *et al.*, 2012, *MNRAS*, 422, 2816
 Bowler, R.A.A., *et al.*, 2012, *MNRAS*, 426, 2772
 Bruzual, G., Charlot, S., 2003, *MNRAS*, 344, 1000
 Cappellari, M., *et al.* 2012, *Nat.*, 484, 485
 Carretero *et al.*, 2004, *ApJ*, 609, L45
 Cimatti, A. *et al.*, 2009, *Exp. Astron.*, 23, 39
 Coelho, P., *et al.*, 2005, *A&A*, 443, 735
 Conroy, C, van Dokkum, P. G., 2012, *ApJ*, 747, 69
 Conroy, C., Graves, G., van Dokkum, P., 2013, arXiv:1303.6629
 Curtis-Lake, E., *et al.*, 2012, *MNRAS*, 422, 1425
 Daddi, E., *et al.*, 2005, *ApJ*, 626, 680
 Daddi, E., *et al.* 2007, *ApJ*, 670, 156
 Dekel, A., *et al.* 2009, *Nat.*, 457, 451
 de La Rosa, I. G., La Barbera, F., Ferreras, I., de Carvalho, R. R., 2011, *MNRAS*, 418, L74
 De Lucia, G., *et al.*, 2006, *MNRAS*, 366, 499
 Dunlop, J. S., 2013, *ASSL*, 396, 223
 Faber, S. M., *et al.*, 2007, *ApJ*, 665, 265
 Fan, X., *et al.*, 2006, *ARA&A*, 44, 415
 Ferreras, I., Charlot, S., Silk, J., 1999, *ApJ*, 512, 81
 Ferreras, I., Pasquali, A., *et al.*, 2012, *AJ*, 144, 47
 Ferreras, I., La Barbera, F., de la Rosa, I. G., Vazdekis, A., *et al.*, 2013, *MNRAS*, 429, L15
 Foley, R. J., Kasen, D., 2011, *ApJ*, 729, 55
 Förster-Schreiber, N.M., *et al.*, 2011, *ApJ*, 739, 45
 Gallazzi, A., *et al.*, 2005, *MNRAS*, 362, 41
 Guo, Q., *et al.*, 2013, *MNRAS*, 428, 1351
 Hewett, P., *et al.*, 2006, *MNRAS*, 367, 454
 Hinshaw, G., *et al.*, 2013, *ApJS*, in press (arXiv:1212.5226)
 Hopkins, A. M., & Beacom, J. F. 2006, *ApJ*, 651, 142
 Hopkins, P. F., 2012, arXiv:1204.2835
 Iliev, I. T., *et al.*, 2012, *MNRAS*, 423, 2222
 Johansson, J., Thomas, D., Maraston, C., 2012, *MNRAS*, 421, 1908
 Jørgensen, I., *et al.*, 2013, *AJ*, 145, 77
 Kauffmann, G., *et al.*, 2003, *MNRAS*, 341, 54
 Kawata, D., Mulchaey, J. S. 2008, *ApJ*, 672, L103
 Khochfar, S., & Silk, J. 2006, *MNRAS*, 370, 902
 Koleva, M., *et al.*, 2008, *MNRAS*, 385, 1998
 Koleva, M., Vazdekis, A., 2012, *A&A*, 538, 143
 La Barbera, F., Ferreras, I., Vazdekis, A., *et al.*, 2013, *MNRAS*, in press, arXiv:1305:2273
 Laureijs, R., *et al.*, 2011, *ESA/SRE(2011)12*, arXiv:1110.3193
 Leonardi, A. J., Rose, J. A., 1996, *AJ*, 111, 182
 Loeb, A., 2013, *ASSL*, 396, 3
 Mandelbaum, R., 2012, *MNRAS*, 420, 1518
 McGee, S., *et al.*, 2011, *MNRAS*, 413, 996
 Milone, A., *et al.*, 2011, *MNRAS*, 414, 1227
 McLure, R. J., *et al.*, 2013, *MNRAS*, in press (arXiv:1212.5222)
 Möller, P., *et al.*, *MNRAS*, in press, arXiv:1301.5013
 Mortlock, A., *et al.*, 2011, *Nature*, 474, 616
 Moster, B., *et al.*, 2010, *ApJ*, 710, 903
 McQuinn, M., *et al.*, 2007, *MNRAS*, 381, 75
 Muzzin, A., *et al.*, 2012, *ApJ*, 746, 188
 Muzzin, A., *et al.*, 2013, *ApJS*, 206,8
 Neistein, E., Li, C., Khochfar, S., *et al.* 2011, *MNRAS*, 416, 1486
 Nakamura, E., *et al.*, 2011, *MNRAS*, 412, 2579
 Oliver, S., *et al.*, 2010, *A&A*, 518, L21
 Ono, Y., *et al.*, 2010, *ApJ*, 724, 1524
 Ouchi, M., *et al.*, 2010, *ApJ*, 723, 869
 Pasquali, A., *et al.*, 2009, *MNRAS*, 394, 38
 Pasquali, A., *et al.*, 2010, *MNRAS*, 407, 937
 Pérez-González, P. G., *et al.*, 2008, *ApJ*, 675, 234
 Pietrinferni, A., *et al.*, 2004, *ApJ*, 612, 168
 Pietrinferni, A., *et al.*, 2006, *ApJ*, 642, 797
 Poggianti, B.M., *et al.*, 2006, *ApJ*, 642, 188
 Pontzen, A, *et al.*, 2008, *MNRAS*, 390, 1349
 Renzini, A., 2006, *ARA&A*, 44, 141
 Richards, G. T., Strauss, M. A., Fan, X., *et al.* 2006, *AJ*, 131, 2766
 Robertson, B. E., *et al.*, 2013, *ApJ*, 768, 71
 Rodighiero, G., Daddi, E., *et al.*, 2011, *ApJ*, 739, L40
 Ryan, R. E., Jr., *et al.*, 2008, *ApJ*, 678, 751
 Schenker, M., *et al.*, 2012, *ApJ*, 744, 179
 Schenker, M., *et al.*, 2013, *ApJ*, 768, 196
 Silk, J., Mamon, G., 2012, *Res. in Astron. & Astrophys.*, 12, 917
 Springel, V., *et al.*, 2005, *Nature*, 435, 629
 Stark, D., *et al.*, 2010, *MNRAS*, 408, 1628
 Thomas, D., *et al.*, 2005, *ApJ*, 621, 673
 Thomas, D., Maraston, C., Johansson, J., 2011, *MNRAS*, 412, 2183
 Tinsley, B., 1980, *Fundam. Cosmic Phys.*, 5, 287
 Toft, S., *et al.*, 2012, *ApJ*, 754, 3
 van den Bosch, F.C., Pasquali, A., *et al.*, 2008, arXiv:0805.0002
 van de Sande, J., *et al.* 2012, arXiv:1211.3424
 van Dokkum, P.G., Conroy, C., 2010, *Nature*, 468, 94
 Vanzella, E., *et al.*, 2011, *ApJ*, 730, L35
 Vazdekis, A., *et al.*, 2003,
 Vazdekis, A., *et al.*, 2010, *MNRAS*, 404, 1639
 Vazdekis, A., *et al.*, 2012, *MNRAS*, 424, 157
 Vulcani, B., *et al.*, 2010, *ApJ*, 710, L1
 Weinmann, S.M., *et al.*, 2006, *MNRAS*, 366, 2
 Weidner, C., Kroupa, P., Pflamm-Altenburg, J., 2011, *MNRAS*, 412, 979
 Wetzel, A.R., Tinker, J.L., Conroy, C., 2012, *MNRAS*, 424, 232
 Wilman, D.J., *et al.*, 2005, *MNRAS*, 358, 71
 Willott, C., *et al.*, 2010, *AJ*, 139, 906
 Woosley, S. E., Heger, A., Weaver, T. A., 2002, *Rev. Mod. Phys.*, 74, 1015
 Worthey, G., 1994, *ApJS*, 95, 107
 York, D. G., *et al.*, 2000, *AJ*, 120, 1579
 Zamkotsian, F. *et al.*, 2010, *Proc. SPIE Vol. 7596*, 75960E